AMPHIBOLE IN THE PORPHYRIES OF THE TIBCHI ANOROGENIC RING-COMPLEX, NIGERIA: PRODUCT OF DEUTERIC ADJUSTMENTS

ECHEFU C. IKE

Department of Geology, Ahmadu Bello University, Zaria, Nigeria

PETER BOWDEN

Department of Geology, University of St. Andrews, St. Andrews, Fife, Scotland KY16 9ST

ROBERT F. MARTIN

Department of Geological Sciences, McGill University, 3450 University Street, Montreal, Quebec H3A 2A7

ABSTRACT

The hydrothermal alteration of porphyries of the Tibchi anorogenic ring-complex, in Nigeria, can be linked to the emplacement and subsequent hydrothermal evolution of the cogenetic biotite granite, the only plutonic phase of the complex. Subsolidus reactions led to the conversion of the primary assemblage of hedenbergitic clinopyroxene and fayalite to amphibole that belongs to either a ferro-actinolite – ferro-edenite trend in the less evolved porphyries, or to a ferro-actinolite – ferro-richterite trend in the more evolved porphyries. The deuteric modifications have partly to completely "reset" the mafic mineralogy of the porphyries. Bulk compositions were also modified: some porphyries have been somewhat silicified, whereas the biotite granite was albitized in its marginal and roof zones by the migrating fluid phase.

Keywords: deuteric reactions, iron-rich amphibole, ferro-hedenbergite, fayalite, Tibchi, Nigeria, anorogenic ring-complex.

SOMMAIRE

L'altération hydrothermale des porphyres du complexe anorogénique de Tibchi (Nigéria) est directement liée à la mise en place et l'évolution hydrothermale subséquente du granite à biotite, seule unité plutonique du complexe. Les réactions subsolidus ont transformé l'assemblage primaire à clinopyroxène hédenbergitique et fayalite à une amphibole qui définit soit une lignée ferro-actinote – ferro-édenite dans les porphyres les moins évolués, soit une lignée ferro-actinote – ferro-richtérite dans ceux qui sont plus évolués. Les modifications deutériques ont partiellement ou complètement remanié les minéraux mafiques des porphyres. La composition globale des roches a aussi été modifiée: certains porphyres ont été quelque peu silicifiés, tandis que le granite à biotite a été albitisé près du toît et des bordures par la phase fluide en circulation.

Mots-clés: réactions deutériques, amphibole ferrifère, ferro-hédenbergite, fayalite, Tibchi (Nigéria), complexe annulaire anorogénique.

INTRODUCTION

The Tibchi ring-complex forms part of the Nigerian Younger Granite province of anorogenic magmatic centres. It is Middle Jurassic [171 $\pm$ 3 Ma, $(^{87}Sr/^{86}Sr)_0 = 0.717 \pm 0.004$; Rahaman *et al.* (1984)] and consists mostly of rocks of granitic composition. The complex is circumscribed by a ring-dyke of granite porphyry; the enclosed mass of biotite granite is asymmetrically disposed with respect to the elliptical ring-dyke (Fig. 1). A plug of quartz porphyry and a suite of related ignimbritic rocks are also found near the western rim. The continuous and narrow ring-dyke formed after cauldron subsidence and partial evacuation of the subvolcanic reservoir by fluidization (Ike 1983). Ike *et al.* (1984) documented the original magmatic assemblage of mafic minerals in these rocks, focusing on the microphenocrysts of fayalite and clinopyroxene. We now shift our attention to the postmagmatic changes that affect the quartz porphyry plug and the granite porphyry ring-dyke, involving the appearance of amphibole after the complete consolidation of the rocks. The Nigerian complexes are type examples of the anorogenic silica-oversaturated igneous complexes; details concerning the relative importance of magmatic and postmagmatic minerals in these rocks can help in the interpretation of similar rocks in more complicated or older intrusive complexes.

The Tibchi complex is ideally suited for an investigation of the subtle postmagmatic changes. Firstly, the structural pattern defined by the map-units is very simple (Fig. 1); volcanic rocks and the porphyries are truncated by biotite granite, which represents the plutonic phase of the complex. Secondly, all rocks emplaced before the biotite granite have a primary assemblage of anhydrous minerals. The subsolidus modifications can be related, by a study of the field relationships, to the emplacement of the biotite granite stock.
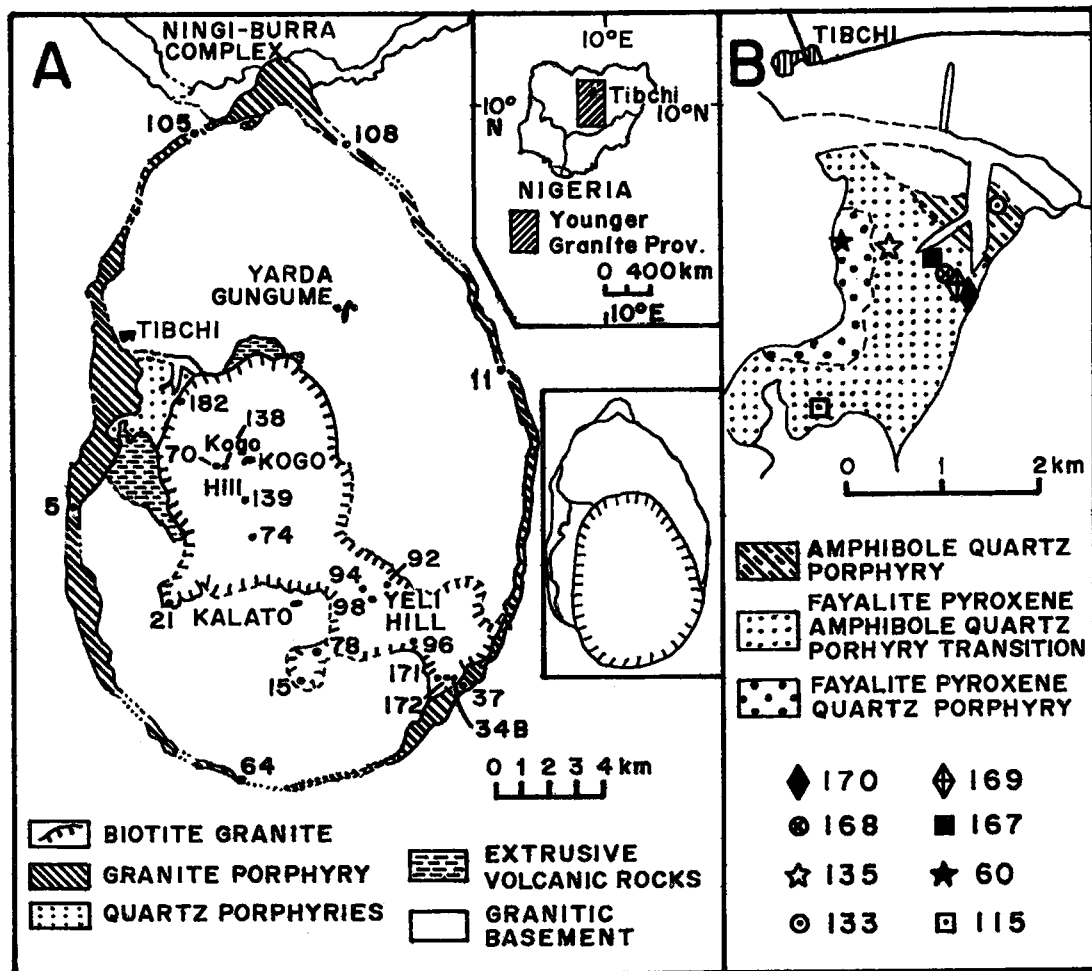
FIG. 1. A. Simplified geological map of the Tibchi complex, showing major rock-units. The ring dyke of granite porphyry overlaps the southernmost portion of the Ningi–Burra complex. The basement complex consists mainly of gneissic granite emplaced during the Pan-African orogeny. The complex was mapped by E.C. Ike. The middle inset shows the inferred outline of the biotite granite in the subsurface; the focus of the granite stock is offset to the south slightly, so that it truncates the ring dyke in the subsurface. B. Expanded view of the area near Tibchi village, showing location of samples referred to in the text. Note that the T prefix has been removed from each sample for clarity.

FIELD RELATIONSHIPS

Quartz porphyry

The plug of quartz porphyry is bounded to the west by the granite porphyry ring-dyke and to the east by the stock of biotite granite. Whereas that part of the plug nearest the ring-dyke is unaltered, the quartz porphyry on the flanks of the biotite granite shows signs of alteration; this increases in intensity as the biotite granite contact is approached. A transition has been mapped between the pristine quartz – fayalite – hedenbergite porphyry and the hydrother-mally modified amphibole-bearing quartz porphyry (Fig. 1).

The clearest indication of the inception of alteration is a change in color of the groundmass, from the usual green to blotches of light blue or grey. The blotches increase in size, and the new color eventually dominates as the contact with biotite granite is approached. Along the contact, variants are found that are totally light blue or grey, without green areas; which color occurs depends on the specific composition of the clinopyroxene and fayalite in the "parent" quartz porphyry, the bluish specimens formerly containing the more evolved composi-

tions of the primary minerals, *e.g.*, the ratio $100Mg/(Mg + Fe^{3+} + Fe^{2+} + Mn)$ approached 0 and the proportion of the acmite component was at its highest in the clinopyroxene (Ike *et al.* 1984). The color change can also be correlated with modifications in the feldspar mineralogy and in the microtexture of the groundmass (see below).

Granite porphyry

Systematic sampling of the ring-dyke by the first author reveals a distinct lithological variation that would be most difficult to explain in terms of magmatic phenomena alone. In the western, northern and northeastern parts of the ring-dyke, the granite porphyry is pristine, but in the southern and southeastern segments, the rock has been modified. The Ca-rich pyroxene normally present is replaced by amphibole, accompanied by sodic pyroxene in one locality where the ring-dyke is very narrow. In the southeastern part, where the contact of the ring-dyke with the biotite granite is exposed, the granite porphyry is extensively modified, just as the quartz porphyry is modified near its contact with the biotite granite.

One may thus conclude that the hydrothermally modified rocks bear a spatial relation to the stock of biotite granite. Ike (1983) proposed that the stock was emplaced during a slight shift in magmatic focus toward the south, *i.e.*, it truncates the vertical ring-dyke in the subsurface in that area. Those parts of the ring-dyke that are underlain by granite can be expected to be thoroughly altered.

Biotite granite

The margin of the biotite granite stock consists of a microgranitic facies, except where the stock abuts against the volcanic rocks and the quartz porphyry plug (in which case there is no decrease in grain size). The area near Kogo Hill in the central part of the complex is also microgranitic. Remnants of microgranite cap some of the hills of biotite granite that encircle the village of Kogo, suggesting that the microgranitic facies is sheet-like and represents the roof of the stock.

PETROGRAPHIC DESCRIPTIONS

We present here a description of the altered rocks in order to document the development of the hydrothermal overprint. The petrography of the pristine parts of the quartz porphyry plug and of the granite porphyry ring-dyke, which are amphibole-free, has been described in detail by Ike *et al.* (1984).

Quartz porphyry

The descriptions are based on samples collected along a traverse (Fig. 1) from T60, the pristine material, to T170, which is directly in contact with biotite granite to the east. In addition, specimens T133, taken to the north of the above traverse, and T115, to the south, are included owing to their unusual light blue color.

The rocks that have light blue blotches contain a ferro-richteritic amphibole that occurs as small reticulate crystals sparsely distributed in the groundmass and as an overgrowth on the microphenocrysts of clinopyroxene. This amphibole may coexist with ferro-actinolite, which forms elongate, fibrous, dull green crystals. Both the phenocryst and groundmass feldspars consist of orthoclase cryptoperthite with an identical composition and degree of Al–Si order, though the extent of turbidity of the K-rich feldspar is clearly greater than in the parent rock. Recrystal-
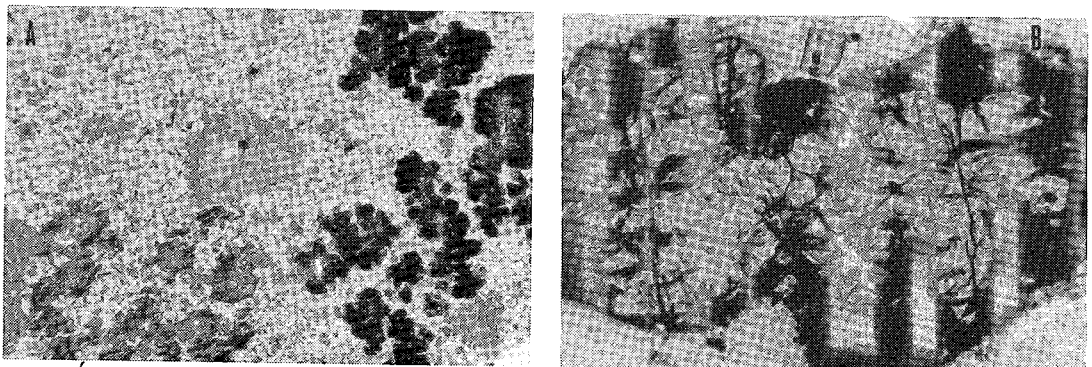

FIG. 2. A. "Needles", "brushes" and "sponges" of ferro-richterite in the groundmass of hydrothermally altered quartz porphyry (specimen T133). Domains of ferro-richterite in each of the two aggregates are in optical continuity. Plane-polarized light; width of field of view: 2 mm. B. Pseudomorph of ferro-richterite encroaching on phenocryst of fayalite. Note the control exerted by fractures on the distribution of the pseudomorph. Riebeckite surrounds small inclusions of ilmenite (*e.g.*, upper left). Quartz porphyry T115. Plane-polarized light; width of field of view: 1.5 mm.

lization of the groundmass has not occurred to any appreciable extent, though the spherulitic clusters seem to have coarsened to varying degrees.

Where the blotches are grey rather than light blue, the clinopyroxene seems intensely altered to poorly defined crystals of the alteration assemblage. Ferro-edenite was detected by microprobe analysis. In other cases, the amphibole is found to consist mainly of anhedral, dull green ferro-actinolite; it coexists with well-formed, turquoise-colored laths of ferro-edenite. In some cases, granular crystals of titaniferous magnetite have precipitated with monazite and fluorite in a ring around a core of ferro-edenite laths.

In advanced stages of alteration, the only mafic phase is ferro-richteritic amphibole, which crystallizes in polycrystalline aggregates of short euhedral prisms closely associated with titaniferous magnetite granules. Each cluster of the two minerals seems to have formed by the complete degradation of a pre-existing microphenocryst of clinopyroxene or fayalite. The ferro-richteritic amphibole is more commonly found as widespread reticulate masses, "sponges", "bristles" and "brushes", and in the groundmass as small scattered crystals (Fig. 2A). The ferro-richteritic amphibole is identified on the basis of its strong pleochroism (α pale yellow, β blue-black, γ dark greenish blue). In well-formed crystals, orientations parallel to the Z axis show anomalous extinction. The ferro-edenite is identified on the basis of its pleochroic scheme (α yellow, β green, γ light turqoise), $\gamma \wedge Z = 23°$, and standard optical properties.

With increasing degree of recrystallization of the groundmass, the extent of turbidity observed in the groundmass feldspar diminishes, but at the same time the phenocrysts of feldspar become progressively more turbid and almost completely brownish. In the most advanced stages (*e.g.*, T170), reorganization of
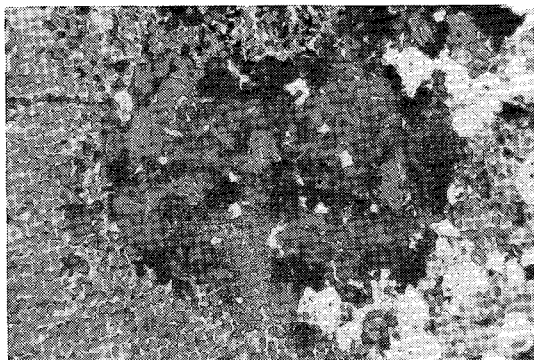

Fig. 3. Polycrystalline aggregate of ferro-edenite crystals formed by the breakdown of a pre-existing phenocryst of clinopyroxene. Granite porphyry from ring-dyke, specimen T37; plane-polarized light. Width of field of view: 2 mm.

TABLE 1. MODAL COMPOSITION OF REPRESENTATIVE BIOTITE GRANITES

	T96	T182	T138	T139
Quartz	31.65	32.46	29.15	35.85
Alkali feldspar	63.75	60.37	52.13	45.99
Plagioclase	0.05	0.49	13.00	13.50
Biotite	4.05	4.85	5.44	4.48
Accessories	0.50	1.83	0.27	0.18

Based on approximately 2300 counts in each case. T96, T182: alkali feldspar granite; T138, T139: plagioclase-bearing mineralized granite from the Kogo Hill area.

the exsolution texture in the phenocrysts has led to readily visible enclaves of polysynthetically twinned albite. At this point, discrete crystals of albite become conspicuous in the groundmass. The boundaries of individual phenocrysts become indistinguishable from the groundmass in plane-polarized light, once the turbidity is removed at the peak of recrystallization of the exsolution texture. At this stage, the groundmass feldspars consist of structurally intermediate microcline (obliquity $\Delta = 0.74$) and pure ordered albite. The acicular ferro-richteritic amphibole in the groundmass is considered contemporaneous with this recrystallization. Where present in the highly modified rocks, the opaque oxides are restricted to the vicinity of the new amphibole.

Specimen T115 is moderately recrystallized and characterized by a green ferro-richteritic rim on fayalite (Fig. 2B). It is unusual in showing indigo-blue riebeckite around inclusions of primary ilmenite in the grains of fayalite.

Granite porphyry

Alteration of the clinopyroxene, increase in degree of Al–Si order in the K-feldspar and progressive recrystallization of the groundmass are the same as observed in the quartz porphyry (above). In addition, in the type locality for highly modified granite porphyry (T37), at the biotite granite contact in the southeastern part of the complex (Fig. 1), ferro-edenitic amphibole is the only mafic mineral (Fig. 3) instead of a ferro-augitic to ferro-hedenbergitic clinopyroxene in the fresh material. Unlike the case of the quartz porphyry, the ferro-edenite here crystallizes not only in polycrystalline aggregates at the expense of the original clinopyroxene, but also as large anhedral crystals whose extensions may penetrate fractures in the quartz and feldspar phenocrysts.

In specimen T64, taken where the granite porphyry is unusually thin and chilled against the Pan-African basement (Fig. 1), polycrystalline aggregates of aegirine-augite seem to replace the original crystals of clinopyroxene, and are in turn replaced along their margin by tufts and wisps of blue amphibole, most likely arfvedsonite. In the groundmass, both acicular blue arfvedsonite and stellate aggregates of aegirine-augite and arfvedsonite are present.

Biotite granite

The biotite granite stock is composed predominantly of a medium-grained alkali feldspar granite in which plagioclase is scarcely found as a discrete phase. However, near the mineralized zone at Kogo Hill, in the centre of the complex, and at Yeli Hill, in the southeast, the modal proportion of sodic plagioclase may attain 13% by volume (Table 1). The typical K-feldspar varies from pink to pale yellow and is characterized by an irregular vein-type intergrowth with albite. Patches of well-twinned albite are also developed within the perthite, in optical continuity with broadly twinned albite at the margin of perthite grains. The quartz typically is strained. The biotite is brownish green except near the contact with volcanic rocks and the quartz porphyry plug, where it is dark grey-green and encloses grains of partly metamict zircon. The fluorite may also be included in or surround biotite, whose cleavage is accentuated by concentrations of hematite. Magnetite in biotite shows oxidation-controlled lamellae of ilmenite and locally is transformed to hematite.

The plagioclase-bearing porphyritic biotite granite of Kogo Hill (T138) hosts numerous greisen veins and lodes in which cassiterite, wolframite, sphalerite, galena, pyrite, arsenopyrite and chalcopyrite may be found. Pink perthite mantles cream-colored plagioclase (An_{26}, Michel-Lévy method). The quartz grains contain numerous dusty inclusions. Biotite is dark brown, strongly pleochroic, crowded with zircon and monazite, and partly chloritized along the cleavage and the edge of the grains. The equigranular groundmass consists of K-feldspar, quartz, albite and biotite.

A cream-colored variant (T70) is found associated with copper sulfides and traces of native copper. This rock contains a greater proportion of secondary albite. The biotite is characteristically reddish brown and invariably altered to chlorite and siderite(?). In specimen T139, the host rock to the Kogo lode, the plagioclase grains are not mantled by perthite, in contrast to T138 and T70. The biotite is green, generally chloritized and associated with hematite and fluorite.

Biotite microgranite

These border or roof-zone rocks are whitish, fine-grained and sparsely porphyritic. Albite predominates in the perthite grains. Biotite varies from brownish green to dark green. In the groundmass, albite and K-feldspar occur as discrete crystals. The rock is locally micrographic in texture and characterized by miarolitic cavities. Accessory phases include fluorite, Fe-Ti oxides, zircon and topaz, the latter prominent in the Kogo Hill area.

WHOLE-ROCK COMPOSITIONS

The composition of selected specimens of porphyry and biotite granite is given in Tables 2 and 3. The differentiation index of all specimens exceeds 80; the compositions can thus be plotted in the haplogranitic system $NaAlSi_3O_8–KAlSi_3O_8–SiO_2$ in order to compare with the data of Tuttle & Bowen (1958) and Luth & Tuttle (1969) concerning minimum-melt and vapor-phase compositions, respectively.

TABLE 2. CHEMICAL COMPOSITION OF THE AMPHIBOLE-BEARING PORPHYRIES, TIBCHI COMPLEX

		T135	T167	T168	T169	T170	T133	T37
SiO_2	wt.%	76.28	75.88	73.37	74.08	77.28	76.49	71.99
TiO_2		0.30	0.20	0.41	0.30	0.10	0.20	0.40
Al_2O_3		10.61	11.04	11.83	11.70	10.41	10.85	12.74
Fe_2O_3		1.13	1.80	2.22	2.35	1.66	1.10	1.75
FeO		1.48	1.30	1.65	1.20	0.78	1.41	2.26
MnO		0.04	0.06	0.08	0.08	0.04	0.05	0.10
MgO		0.03	0.09	0.10	0.14	0.03	0.02	0.14
CaO		0.46	0.54	0.73	0.80	0.26	0.33	1.04
Na_2O		4.12	3.85	3.88	4.00	3.55	4.08	4.02
K_2O		4.91	4.83	5.02	4.89	4.77	4.85	5.17
P_2O_5		0.02	0.01	0.01	0.01	0.01	0.00	0.06
H_2O^+		0.25	0.50	0.46	0.49	0.29	0.18	0.27
H_2O^-		0.11	0.10	0.14	0.15	0.09	0.04	0.05
Total		99.74	100.20	99.90	100.19	99.27	99.62	99.99
A.I.		1.14	1.05	1.00	1.01	1.06	1.11	0.95
D.I.		91.32	92.75	92.86	93.06	93.62	92.23	90.82

Specimens: T135, T167, T168, T169, T170, T133: quartz porphyry; T37: granite porphyry, sampled from the ring-dyke. A.I. agpaitic index, D.I. differentiation index. Analysts: R.A. Batchelor and E.C. Ike. Analyses by atomic absorption. For bulk composition of more pristine specimens of quartz porphyry and granite porphyry, see Ike et al. (1984, Table 1).

TABLE 3. CHEMICAL COMPOSITION OF REPRESENTATIVE SPECIMENS OF BIOTITE GRANITE, TIBCHI COMPLEX

		T171	T172	T34B	T96	T58	T182	T92	T92V[1]	T94	T98	T138	T70	T139	T15A	T78	T21	T74
SiO_2	wt.%	77.40	77.21	76.90	77.60	77.70	77.14	76.30	74.91	76.60	78.72	74.80	76.10	75.60	77.00	77.33	76.90	77.86
TiO_2		0.09	0.08	0.10	0.05	0.05	0.10	0.10	0.05	0.07	0.09	0.20	0.07	0.05	0.08	0.01	0.05	0.10
Al_2O_3		11.79	12.01	11.35	11.29	11.29	12.12	12.06	12.23	11.95	11.45	12.10	12.18	12.26	11.74	11.41	11.50	11.85
Fe_2O_3		0.59	0.76	0.17	0.17	0.24	0.48	0.30	0.81	1.00	1.17	0.73	0.14	0.31	0.89	0.20	0.37	0.08
FeO		0.67	0.65	0.94	1.03	1.08	0.69	0.86	1.30	0.37	0.00	2.12	1.24	1.31	0.89	0.20	0.91	0.94
MnO		0.02	0.03	0.02	0.02	0.02	0.02	0.02	0.03	0.02	0.02	0.04	0.03	0.02	0.02	0.02	0.03	0.03
MgO		0.03	0.03	0.02	0.04	0.02	0.03	0.02	0.05	0.05	0.09	0.08	0.03	0.02	0.01	0.05	0.03	0.02
CaO		0.45	0.57	0.46	0.62	0.39	0.46	0.50	0.90	0.63	0.44	0.85	0.58	0.62	0.26	0.40	0.51	0.47
Na_2O		3.68	3.86	4.16	3.78	3.56	3.83	3.52	4.60	3.43	3.20	3.23	3.61	3.15	3.88	4.15	4.06	4.45
K_2O		4.69	4.58	4.58	4.63	4.36	4.55	4.74	4.48	4.64	4.81	4.41	4.45	4.55	4.59	4.32	4.53	4.26
P_2O_5		0.01	0.00	0.00	0.00	0.02	0.00	0.00	0.00	0.00	0.01	0.00	0.00	0.00	0.00	0.00	0.00	0.00
H_2O^+		0.53	0.42	0.38	0.36	0.85	0.44	1.07	0.30	0.20	0.51	0.42	0.64	1.02	0.59	0.42	0.28	0.39
H_2O^-		0.13	0.10	0.18	0.12	0.05	0.12	0.08	0.08	0.12	0.09	0.08	0.10	0.10	0.11	0.06	0.10	0.05
Total		100.08	100.30	99.36	99.71	100.13	99.95	99.57	99.74	99.08	100.60	99.06	99.17	98.91	99.50	99.49	99.27	100.50
A.I.		0.94	0.94	1.05	1.00	0.89	0.92	0.91	1.02	0.89	0.92	0.83	0.88	0.83	0.97	1.01	1.01	1.01
D.I.		95.70	95.66	94.98	95.70	94.59	95.36	93.82	93.76	93.90	96.15	89.20	92.67	91.05	95.72	96.44	95.50	96.96

Specimens: T171, T172, T34B, T96: biotite granite, southeastern sector; T58, T182: biotite granite, northwestern sector; T92, T92V[1], T94, T98: biotite granite, Yeli Hill sector; T138, T70, T139: biotite granite, Kogo Hill sector; T15A, T78, T21, T74: marginal and roof-zone microgranite. A.I. agpaitic index, D.I. differentiation index. Analysts: R.A. Batchelor and E.C. Ike. Analyses by atomic absorption.

Most of the felsic rocks of the Tibchi complex plot in the central portion of the haplogranite system (Fig. 4), in the "terminal" part of the field defined by granites and syenites of the Nigerian suites (Bowden & Turner 1974). The hydrothermally altered porphyries define a linear trend consistent with a progressive increase (or decrease) in normative quartz, relative to the position of the pristine specimens, presumably close to the water-saturated mini-mum in the granite system at 1 kbar (shown in Fig. 4B). The unmineralized samples of biotite granite occupy an intermediate position between the specimens of mineralized granite, which are richer in normative quartz and depleted in normative albite, and those of biotite microgranite, which are richer in normative albite (Fig. 4B). The hydrothermal modification of the intrusive rocks and the mineralization of the biotite granite lead to increased normative
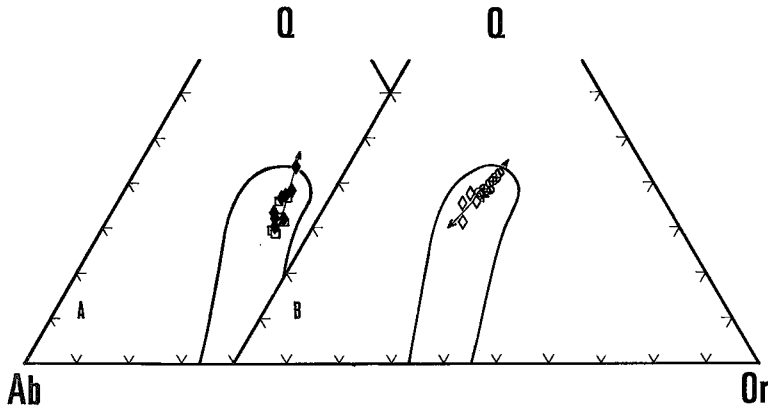

FIG. 4. Compositional trends in the porphyries (A) and biotite granite and microgranite (B) at Tibchi, in terms of normative quartz (top), albite (Ab) and K-feldspar (Or) components. Filled diamond: quartz porphyry, open square: granite porphyry (ring-dyke material), open circle: biotite granite, circle with cross: mineralized biotite granite (Kogo Hill locality), circle with diagonal: mineralized plagioclase-bearing biotite granite (Yeli Hill locality), open diamond: biotite microgranite. The + marks the location of the water-saturated minimum in the granite system at 1 kbar (Tuttle & Bowen 1958). Also shown is the compositional envelope defined by the syenitic and granitic rocks of Niger and Nigeria (Bowden & Turner 1974).

TABLE 4. REPRESENTATIVE COMPOSITIONS OF AMPHIBOLES, TIBCHI COMPLEX

		1	2	3	4	5A	5B	6	7A	7B	7D	8	9	10A	10B	11	12
SiO_2	wt.%	46.82	44.23	43.25	41.10	42.04	44.04	46.60	48.73	47.68	46.59	47.89	49.23	47.41	47.84	46.30	50.21
TiO_2		0.15	0.11	0.27	1.30	1.32	1.03	0.51	0.14	0.81	1.23	1.26	0.93	1.49	1.40	1.26	0.05
Al_2O_3		2.46	3.47	6.07	6.06	6.22	5.39	1.18	0.75	1.56	1.91	1.20	1.13	1.52	1.42	3.80	0.09
Fe_2O_3		0.57	1.98	1.19	0.00	0.00	0.00	0.00	0.00	0.00	0.00	0.00	0.00	0.00	0.00	0.00	10.15
FeO		31.44	31.13	31.64	33.94	32.91	32.98	34.35	34.56	34.32	34.22	34.80	36.03	34.24	33.80	33.23	28.71
MnO		1.23	1.99	1.05	0.50	0.78	0.89	0.00	1.50	0.96	0.87	0.68	0.38	0.75	0.54	0.20	0.42
MgO		2.37	1.36	1.49	1.17	1.80	2.16	0.40	0.36	0.44	0.31	0.34	0.61	0.14	0.15	0.13	0.24
CaO		10.92	10.42	10.65	9.84	10.08	9.88	6.76	7.79	6.61	5.84	4.85	2.78	4.45	3.69	3.35	1.24
Na_2O		0.67	0.96	1.34	2.06	2.06	1.64	3.00	2.15	3.47	4.10	5.01	5.14	5.12	5.44	4.88	6.38
K_2O		0.41	0.46	0.87	1.00	1.20	1.04	0.83	0.36	0.80	1.06	1.11	0.82	1.20	1.22	2.55	0.00
Total		97.04	96.11	97.82	96.97	98.41	99.05	93.63	96.34	96.65	96.13	97.14	97.05	96.32	95.50	95.70	97.48
FeO(T)		31.95	32.91	32.71	33.94	32.91	32.98	34.35	34.56	34.32	34.22	34.80	36.03	34.24	33.80	33.23	37.84
Si*		7.567	7.312	7.014	7.820	6.833	7.057	7.877	7.986	7.808	7.702	7.826	7.990	7.803	7.902	7.644	8.000
^{iv}Al		0.433	0.676	0.986	1.180	1.167	0.943	0.123	0.011	0.192	0.298	0.174	0.010	0.197	0.098	0.356	-
^{vi}Al		0.035	-	0.175	0.005	0.026	0.075	0.113	0.129	0 109	0.075	0.057	0.206	0.099	0.178	0.383	0.018
Fe^{3+}		0.070	0.246	0.145	-	-	-	-	-	-	-	-	-	-	-	-	1.218
Ti		0.018	0.013	0.033	0.163	0.161	0.124	0.065	0.017	0.100	0.153	0.155	0.114	0.185	0.174	0.156	0.006
Mg		0.570	0.336	0.361	0.290	0.436	0.516	0.101	0.088	0.107	0.076	0.084	0.149	0.035	0.037	0.033	0.058
Fe^{2+}		4.143	4.137	4.147	4.475	4.275	4.171	4.721	4.566	4.555	4.578	4.613	4.484	4.579	4.537	4.402	3.647
Mn		0.168	0.268	0.139	0.067	0.102	0.114	-	0.200	0.129	0.118	0.091	0.047	0.102	0.074	0.026	0.053
Fe^{2+}		0.106	0.167	0.145	0.236	0.199	0.248	0.135	0.171	0.144	0.152	0.143	0.407	0.135	0.131	0.186	0.179
Mn		0.004	0.011	0.005	0.004	0.005	0.007	-	0.008	0.004	0.004	0.003	0.005	0.003	0.002	0.001	0.003
Ca		1.890	1.822	1.850	1.748	1.755	1.696	1.225	1.367	1.159	1.034	0.848	0.483	0.785	0.653	0.592	0.212
Na		-	-	-	0.012	0.041	0.049	0.640	0.454	0.693	0.810	1.006	1.105	1.077	1.214	1.221	1.606
Ca		0.001	0.023	0.001	-	-	-	-	-	-	-	-	-	-	-	-	-
Na		0.210	0.307	0.421	0.651	0.608	0.460	0.343	0.228	0.409	0.503	0.582	0.514	0.556	0.528	0.342	0.364
K		0.084	0.096	0.179	0.211	0.248	0.212	0.179	0.075	0.525	0.224	0.232	0.169	0.252	0.257	0.537	-

Specimens: 1 ferro-actinolite, quartz porphyry T169, 2 ferro-actinolitic hornblende, quartz porphyry T169, 3 ferro-edenite from quartz porphyry T169, 4 ferro-edenite, quartz porphyry T168, 5A, 5B zoned ferro-edenite, granite porphyry T37, 6 silicic ferro-edenite, quartz porphyry T170, 7A, 7B, 7D zoned ferro-actinolite with rim of ferro-richterite, quartz porphyry T170, 8 ferro-richterite crystallized along fracture in alkali feldspar phenocryst, quartz porphyry T115, 9 ferro-richterite associated with riebeckite in fayalite phenocryst (see text), quartz porphyry T115, 10A, 10B zoned spongy "porphyroblast" of ferro-richterite, quartz porphyry T133, 11 ferro-richterite nucleated on and growing into pre-existing alkali feldspar phenocryst, quartz porphyry T133, 12 riebeckite surrounding inclusion of ilmenite in partly altered fayalite, quartz porphyry T115. Amphiboles 1 to 7D are calcic, 8 to 11 are sodic-calcic, according to Leake's (1978) classification. Number 12 is an alkali amphibole. Compositions obtained from electron-microprobe data (E.C. Ike, analyst). Structural formulae are calculated on an anhydrous basis, assuming 23 atoms of oxygen, using the procedure of Papike *et al.* (1974). The proportion of ferrous and ferric iron is calculated using charge-balance considerations. Details of the electron-microprobe analytical procedure are provided by Ike *et al.* (1984). * Cations are grouped according to the general formula $A_{0-1}B_2C_5T_8O_{22}(OH,F,Cl)_2$.

quartz and K-feldspar relative to albite, in marked contrast to the progressive increase in Na along the microgranite trend.

AMPHIBOLE COMPOSITIONS

With the exception of the riebeckite associated with fayalite and ilmenite, the compositions in Table 4 correspond to amphiboles in the calcic and sodic-calcic groups (Leake 1978). A plot of $(Na + K)_A$ *versus* (8 – Si) (Ike 1979) can be used to illustrate the compositions of the relatively aluminous and magnesian calcic amphiboles. The thirteen data-points obtained (quartz porphyry specimens T168 and T169, granite porphyry T37) have a ratio 100 $Mg/(Mg + Fe^{3+} + Fe^{2+} + Mn)$ between 11.3 and 5.7 and range from ferro-actinolite to ferro-edenite. A zoned crystal of ferro-edenite from the granite porphyry shows an outward increase in $(Na + K)_A$ and ^{IV}Al along the same trend as defined by the bulk composition of the unzoned grains.

A different trend is followed by those zoned grains of amphibole found in quartz porphyry T170. These compositions are very poor in aluminum and magnesium: [100 $Mg/(Mg + Fe^{3+} + Fe^{2+} + Mn) < 2$], and define a trend from ferro-actinolite to silicic ferro-edenite. A plot of $(Na + K)_A$ *versus* Na_B (Ike 1979) is more appropriate in this case because it shows that the trend of subaluminous compositions defined by T170 evolves beyond the silicic ferro-edenite field to ferro-richterite. The amphibole compositions found in two specimens of quartz porphyry (T115, T133) define a cluster of points in the ferro-richterite field; Na reaches 1.22 a.p.f.u. in the most evolved composition. In T115, ferro-richterite, which locally formed at the expense of fayalite, coexists with riebeckite associated with inclusions of ilmenite in the fayalite.

The collection of amphibole compositions define a continuum between Ca-rich, Na-poor and Na-rich, Ca-poor extremes in a triangular plot Na – Ca – K (with K increasing from less than 5 to approximately 10 atomic % in this sequence). More informative, however, is a plot of Ca *versus* the sum of Na and K (Fig. 5). Three distinct groupings are evident: (1) the ferro-actinolite – ferro-edenite trend, considered
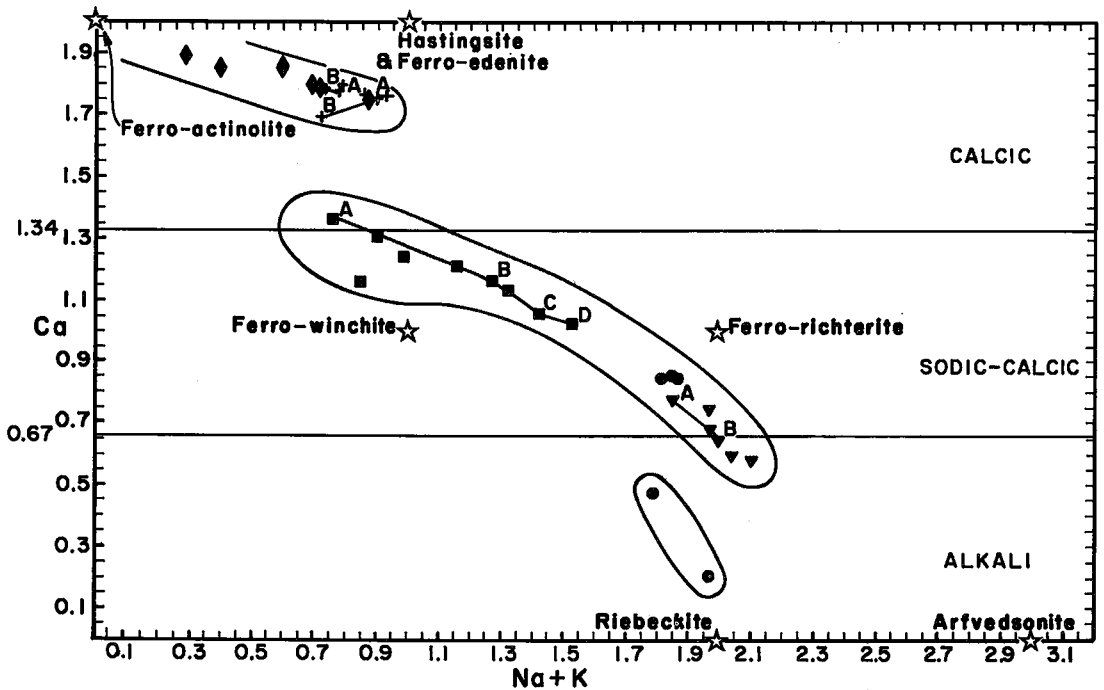
FIG. 5. Composition of the amphiboles in the hydrothermally affected porphyries of the Tibchi Complex, expressed
in terms of (Na + K) *versus* Ca content (cations per formula unit). The compositions define three groupings: (1)
Ca-rich, relatively aluminous ferro-actinolite – ferro-edenite series (diamond: quartz porphyry T169, cross: granite
porphyry T37); (2) relatively Ca-poor, Al-poor ferro-actinolite – ferro-richterite series, tending to arfvedsonite (square:
quartz porphyry T170, circle: quartz porphyry T115, inverted triangle: quartz porphyry T133); (3) alkali-enriched
compositions tending to riebeckite, developed in quartz porphyry T115 around ilmenite grains included in fayalite
microphenocrysts. Each tie-line joins compositions in a zoned crystal: A (core) to B (rim) or A (core) through B
and C to D (rim). Stars mark the composition of the end members.

to originate at the expense of the relatively magne-
sian primary clinopyroxene and olivine; (2) the ferro-
actinolite – ferro-richterite trend, considerably less
calcic and less magnesian, considered to originate at
the expense of the compositionally more evolved
primary clinopyroxene and olivine (Ike *et al.* 1984);
(3) two compositions in the field of alkali amphibole,
the result of a very local buildup of Na. In the second
group, the linear trend defined by bulk compositions
of unzoned grains is the same as that defined by
strongly zoned crystals (see caption to Fig. 5). Note
that all the compositions are close to the iron-bearing
end-members of the respective solid-solution series.

DISCUSSION

The hydrothermal overprint

Luth & Tuttle (1969) determined the composition
of the aqueous vapor phase coexisting with compo-
sitions in the haplogranite system. They showed that
the vapor phase coexisting with quartz and (Na,K)-
feldspar at low confining pressures and 25°C below
the solidus is significantly enriched in normative
quartz relative to the bulk composition of the solid
assemblage. However, 25°C above the solidus, the
vapor phase tends to show increased normative
quartz and albite relative to the coexisting melt,
provided that the coexisting alkali feldspar is
potassic.

In view of these experimental data, the alteration
of the porphyries can best be explained as a conse-
quence of the permeation of these rocks by a vapor
phase preferentially enriched in silica, and emanat-
ing from the nearby stock of biotite granite at a high
subsolidus temperature. The relatively high temper-
ature of the process would be consistent with the field
observation that the biotite granite did not chill
against the porphyries and the volcanic rocks, which
were still cooling, although it did so against the base-
ment rocks. On the other hand, relative albitization
and desilication in the microgranite can be expected
to result from the interaction of roof-zone rocks with
a vapor phase bubbling upward through a column

of crystallizing granitic magma. The development of miarolitic cavities in the granite attests to the saturation of the melt in water, at least locally. Thus some of the water responsible for these mineralogical and textural adjustments was magmatic in origin, the result of progressive buildup through protracted crystallization of dominantly anhydrous minerals. In view of the shallow depth and subsolidus temperature of the interaction, however, some of the water may well represent heated groundwater.

The reactions that produced amphibole

Those specimens of porphyry that show an incomplete replacement of clinopyroxene and fayalite by amphibole show that the amphibole originated at the expense of those two anhydrous minerals. Our data and observations are consistent with an origin by dissolution and local reprecipitation of the newly formed phase. In some cases, the early product is ferro-actinolite; it evidently did not remain in its field of stability, as it gives way in zoned grains to ferro-edenite or ferro-richterite. These two amphiboles do not coexist in the Tibchi suite; which trend is followed seems to depend mainly on the composition of the primary assemblage. The progression in amphibole compositions is well documented in the data bearing on discrete as well as zoned crystals (Fig. 5).

The breakdown of the relatively magnesian clinopyroxene to ferro-actinolite may be represented ideally by the following equation: $5\ Ca(Fe_{0.9}Mg_{0.1})Si_2O_6 + H_2O = Ca_2(Fe_{0.9}Mg_{0.1})_5 Si_8O_{22}(OH)_2 + [3\ CaO + 2\ SiO_2]$. The whitish mineral that occurs as an intrafasciculate phase with the ferro-actinolite may be wollastonite, representing the constituents placed in brackets. Implicit in the idealized reaction proposed is the notion that not much is removed from the site of reaction in the early stages. However, there is evidence that the ferro-actinolite eventually reacted with the adjacent alkali-bearing groundmass assemblage; note that the grains of perthite were probably undergoing a Na-for-K ion-exchange reaction as the transformation to amphibole was occurring. An idealized reaction of relevance could be of the type: $NaAlSi_3O_8$ (groundmass albite) + $Ca_2(Fe_{0.9}Mg_{0.1})_5Si_8O_{22}(OH)_2 = NaCa_2(Fe_{0.9}Mg_{0.1})AlSi_7O_{22}(OH)_2$ (ferro-edenite) + $4SiO_2$. This reaction is consistent with the "edenite" substitution documented by Grapes & Graham (1978): $(Na + K)_A + {}^{IV}Al$ substitutes for $\square_A + {}^{IV}Si$ in ferro-actinolite. This is the predominant scheme of substitution in calcic amphiboles from SiO_2-oversaturated anorogenic ring-complexes the world over (Giret et al. 1980).

The ferro-actinolite – ferro-richterite trend that developed at the expense of pyroxene and olivine in the more evolved, less magnesian rocks may well be

a reflection of the substitution scheme $(Na_A + Na_B) = (\square_A + Ca_B)$ in ferro-actinolite, according to the ion-exchange reaction: $Ca_2(Fe_{0.98}Mg_{0.02})Si_8O_{22}(OH)_2 + 2Na^+ = NaCaNa(Fe_{0.98}Mg_{0.02})_5Si_8O_{22}(OH)_2 + Ca^{2+}$. The maximum thermal stability of such a ferro-richterite composition can be considered to be that determined experimentally for the magnesium-free end-member. At one kilobar $P(H_2O)$ and an oxygen fugacity defined by the quartz – fayalite – magnetite buffer, Charles (1977) found ferro-richterite to be stable below 535 ± 10°C. The observed sequence of changes, first to ferro-actinolite and then, at a more advanced stage, to ferro-richterite, may thus have occurred as a deuteric adjustment as the rock cooled from its solidus temperature, near 800°C (Ike et al. 1984) to a temperature below 535°C, where it entered the field of stability of the alkali-enriched iron-rich amphibole. The QFM buffer seems the most appropriate for the Tibchi complex; in some units, all three phases are present.

At the magmatic stage, the Tibchi complex can be characterized by a consistently low value of oxygen fugacity. The reducing environment seems to have been maintained during the postmagmatic reactions, which led to ferro-edenite and ferro-richterite end-products. This in turn would be consistent with a high ratio of cooling rock to circulating water, and a high proportion of magmatically derived water to infiltrated meteoric water in the circulating system.

Whereas the evidence is unambiguous that amphibole is a primary phenocryst phase in calcalkaline magmas, characterized by relatively high concentrations of Ca, Al and Mg and higher $P(H_2O)$, the timing of amphibole crystallization in low-calcium, very iron-enriched (relative to magnesium) granitic systems emplaced near the earth's surface is considerably less certain. The approach used here, of choosing a simple annular dyke and related conduits, which have been filled by one batch of magma during one event of cauldron subsidence, can provide clear indications that the amphibole made its appearance while the rock cooled. The mineralogical changes were caused by an interaction with an aqueous fluid that left few bulk compositions intact.

REFERENCES

BOWDEN, P. & TURNER, D.C. (1974): Paralkaline and associated ring-complexes in the Nigeria – Niger province, West Africa. *In* The Alkaline Rocks (H. Sorensen, ed.). J. Wiley & Sons, London.

CHARLES, R.W. (1977): The phase equilibria of inter-mediate compositions on the pseudobinary $Na_2CaMg_5Si_8O_{22}(OH)_2$ – $Na_2CaFe_5Si_8O_{22}(OH)_2$. *Amer. J. Sci.* **227,** 594-625.

GIRET, A., BONIN, B. & LEGER, J.-M. (1980): Amphi-bole compositional trends in oversaturated and undersaturated alkaline plutonic ring-complexes. *Can. Mineral.* **18,** 481-495.

GRAPES, R.H. & GRAHAM, C.M. (1978): The actinolite – hornblende series in metabasites and the so-called miscibility gap: a review. *Lithos* **11,** 85-97.

IKE, E.C. (1979): *The Structure, Petrology and Geochemistry of the Tibchi Younger Granite Ring-Complex, Nigeria.* Ph.D. thesis, University of St. Andrews, St. Andrews, Scotland.

_____ (1983): The structural evolution of the Tibchi ring-complex: a case study for the Nigeria Younger Granite province. *J. Geol. Soc. Lond.* **140,** 781-788.

_____, BOWDEN, P. & MARTIN, R.F. (1984): Fayalite and clinopyroxene in the porphyries of the Tibchi anorogenic ring-complex, Nigeria; postmagmatic initiation of a peralkaline trend. *Can. Mineral.* **22,** 401-409.

LEAKE, B.E. (1978): Nomenclature of amphiboles. *Can. Mineral.* **16,** 501-520.

LUTH, W.C. & TUTTLE, O.F. (1969): The hydrous vapour phase in equilibrium with granite and granite magmas. *Geol. Soc. Amer. Mem.* **115,** 513-548.

PAPIKE, J.J., CAMERON, K.L. & BALDWIN, K. (1974): Amphiboles and pyroxenes: characterization of *other* than quadrilateral components and estimates of ferric iron content from microprobe data. *Geol. Soc. Amer. Abstr. Programs* **6,** 1053-1054.

RAHAMAN, M.A., VAN BREEMEN, O., BOWDEN, P. & BEN-NETT, J.N. (1984): Age migrations of anorogenic ring complexes in northern Nigeria. *J. Geol.* **92,** 173-184.

TUTTLE, O.F. & BOWEN, N.L. (1958): Origin of granite in the light of experimental studies in the system $NaAlSi_3O_8$ – $KAlSi_3O_8$ – SiO_2 – H_2O. *Geol. Soc. Amer. Mem.* **74.**